Synthesis of Sparse Circular-Arc Arrays with Wide Angle Scanning Based on Iterative Convex Optimization

Zhenfang Gu, Shiwen Lei, Ziyuan He, Zhipeng Lin, Bo Chen and Qi Xie

University of Electronic Science and Technology of China

Abstract

An iterative convex optimization algorithm for wide scanning sparse conformal array synthesis is proposed. Combined with the compressed sensing (CS) theory, the proposed method is used to find the optimal element position for multiple scanning angle patterns by using cooperative synthesis strategy.

The iterative algorithm first uses Euler's calculation transformation to overcome the problem that the element pattern cannot be superimposed in a unified coordinate system due to the different distribution positions of the array elements.

Secondly, the non-convex sparsity problem of circular-arc array with limited main-lobe width is transformed into a convex form with minimized l1 norm. Several numerical simulations are operated to validate the correctness and effectiveness of the proposed algorithm.

Introduction

Sparse arrays have been widely used in radar systems, satellite communication, radio astronomy and other fields. The sparse array not only reduces the cost by reducing the number of array elements, but also reduces the sidelobe level of the array through the selection of array elements.

In this paper, a method based on iterative convex optimization is proposed to synthesize a scannable sparse conformal array. By using the priori information that different modes should share the same active antenna elements, the method not only considers the different array element pointing problems caused by the influence of carrier curvature, but also considers the correlation between modes. A reasonable tradeoff is achieved between the number of active antenna elements and the pattern characteristics. The wide angle scanning of circular conformal sparse array is completed.

Antenna array theory

As shown in Fig.1, N antenna elements with equal angles are distributed on a ring of radius R and placed tangentially to the ring. The pattern F of the circular ring conformal array can be represented by：

$$F(\varphi,\theta)=\sum_n A_n f_n(\varphi,\theta)e^{j[\alpha_n - kR\cos(\varphi-\varphi_n)\sin(\theta)]}$$

$$k = 2\pi/\lambda$$

Fig.1

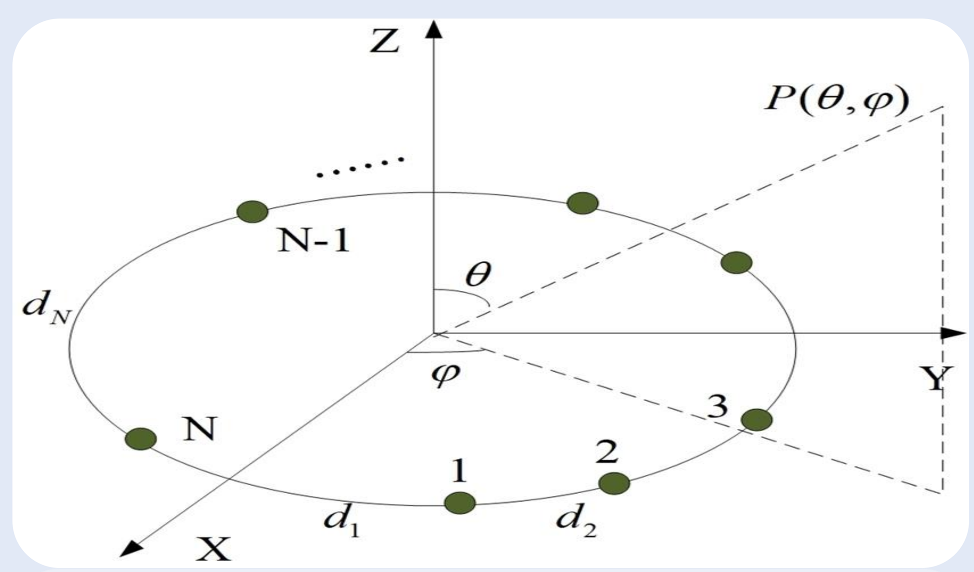

Mathematical model

Making a sparse ring array with wide-angle scanning capability is to reduce the array elements, but also need to consider the multi-mode pattern, which requires finding the common position of the desired multi-beam pattern. Each array element is closely related to a number of directional diagrams with different directions. Only when the related multiple excitations are small enough, can it represent that the necessity of this array element is low and it can be discarded.

$$\min \sum_{m=1}^{M}\frac{|\delta_m|^{t+1}}{|\delta_m|^{t}+\mu}$$

$$s.t.\begin{cases}\delta_m \ge \max\{|a_{1m}|,|a_{2m}|,\cdots,|a_{Lm}|\}\\ \left|p(\varphi)^T a_l\right| \le psll, \varphi\in\phi_l \\ \left|p(\varphi_0)^T a_l\right| == 1 \\ (l=1,2,\cdots,L)\end{cases}$$

Simulation results

Simulation 1:

In Fig.2, the blue curve and the black curve respectively represent the results before and after Euler rotation transformation, and the red curve represents the results of full array simulation using HFSS.The pattern obtained through coordinate transformation and superposition is relatively close to the pattern of the actual simulation, which proves the effectiveness and correctness of the method.

Fig. 2

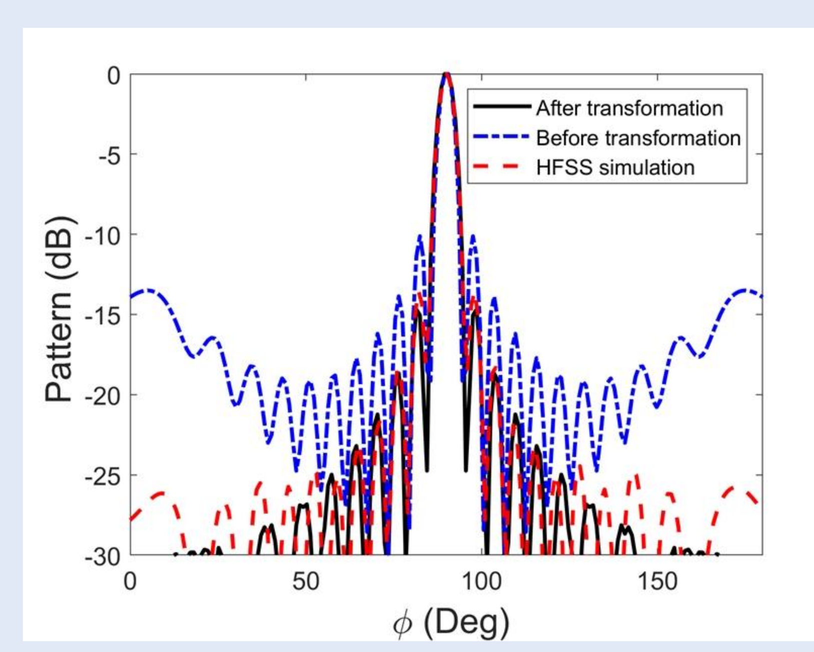

Simulation 2:

The conformal single-beam array is sparsed, and the Euler rotation transform is used to synthesize the array pattern, and the sparse result is compared with other algorithms.

Fig. 3

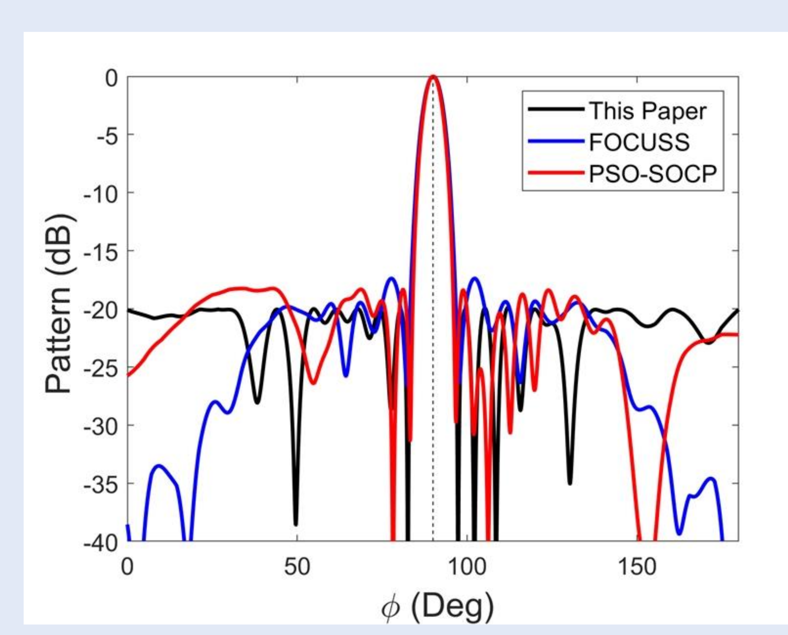

Simulation 3:

The desired multi-beam pattern contains 19 beams, the beam spacing is 5°, the main lobe width is set to 15°, and the maximum sidelobe level of each beam is −20 dB. Through the algorithm of this paper, find the least common element position that produces the required multi-beam pattern. There are 19 array element positions, and the integrated beam pattern is shown in Fig 4.

Fig. 4